International Journal of Mathematics and Statistics Invention (IJMSI)
E-ISSN: 2321 – 4767 P-ISSN: 2321 - 4759
www.ijmsi.org Volume 3 Issue 5 || July. 2015 || PP-26-33

The Effect of Radiation on the Convective Heat and Mass Transfer Flow of a Viscous Electrically Conducted Fluid in a Horizontal Rotating Channel in the Presence of Constant Heat Sources.

Dr.M.Balasubrahmanyam[1] , R. Siva Prasad [2]
[1]*Asst.professor, Dept.of Mathematics,Sri RamakrishnaP.G.College,Nandyal,India*
[2]*Professor, Dept. of Mathematics, S.K.University, Anantapuram, India*

ABSTRACT : *In this paper we have analyzed the effect of radiation on the convective heat and mass transfer flow of a viscous electrically conducted fluid in a horizontal rotating channel in the presence of constant heat sources. The governing partial differential equations can be transformed into a system of ordinary differential equations using non - dimensional process. The velocity, temperature and concentration profiles are shown in graphically for different values of the parameters entering into the problem*

Keywords: *Mixed convective, Heat and mass transfer, Magnetic field, viscous dissipation ,Radiation , constant heat source*

I. INTRODUCTION

Convective flow through porous media is an area of research undergoing rapid a growth in the fluid mechanics and heat transfer field due to its broad range of scientific and engineering applications. It is associated with petroleum and geothermal processes, fiber and granular insulation materials, high performance insulation buildings, transpiration cooling packed bed, chemical reactors control of pollutant spread in ground water. A nice review about heat transfer in geothermal system has been presented in chang [1978].

All fluid phenomena on earth involve rotation to a greater or lesser extent because of the basic rotation of the earth. Most of the large scale motions in atmosphere and seas/oceans fall under the category in which rotation is an absolutely essential factor the atmosphere and the ocean are not homogeneous in compressible fluids, but in many cases the essential physical features of atmospheric or oceanic flows are not dependent on this factor and satisfactory theories can be based on Mathematical models assuming the fluid as incompressible.

A large variety of processes of interest to industry and society involve the flow of fluids through porous media. Examples include the use of filtration to purity water and treat Sewage, Membranes to separate gases, the chemical factors having porous a catalysts supports. The mathematical modeling and simulation of the flow of fluids through porous media are important for designing and controlling a number of industrial processes including the production of fluids from underground reservoir and remediation of under ground water resources fluids embedded in the earth's crust enables one to use minimal energy to extract the minerals. For example, in the recovery of hydrocarbons from underground petroleum reservoirs, the use of thermal processes is becoming important to enhance the recovery. Heat can be injected into the reservoir as hot water or steam, or heat can be generated inside by burning part of the reservoir crude. In all such thermal recovery processes, fluid flow takes place through a porous medium and convection flow through a porous medium is of utmost important. Determination of the external energy required to initiate convection currents needs a though understanding of convective processes in a porous medium. There has been a great quest in Geophysicists to study the problem of convection currents in a porous medium heated from below.

In the last several years considerable attention has been given to the study of the Hydromagnetic thermal convection due to its numerous applications in Geophysical and Astrophysics.In geothermal region gases are electrically conducting and that they undergo the influence of a magnetic field. Magneto-thermal dynamics phenomenon in a porous medium results from the mutual effects of a magnetic field and conducting fluid flowing through the porous medium Examination of the flow model reveals the combined influence of porosity and a magnetic field on the velocity, temperature profiles and the local heat transfer etc.

The unsteady hydromagnetic rotating viscous flow through a porous medium has drawn the attention in recent years for possible applications in Geophysical and Cosmical fluid dynamics. The buoyancy and rotational forces are often comparable in geophysical processes like 'Dust devils' caused by rotating atmosphere above a locally heated surface and other rising atmospheric circulations [2008 &1998]. They are also common in Nature and in devices and processes equipments.

One of the earlier investigation related to this aspect appears in the work of Claire Jacobs [1971] who has studied the transient effects considering the small amplitude torsional oscillations of disks. This problem has been extended to the hydromagnetics by Murthy [1979] who discussed torsional oscillations of the disks maintained at different temperatures. Debnath [1975] has considered an unsteady hydrodynamic and hydromagnetic boundary flow in a rotating, viscous fluid due to oscillations of plates including the effects of the velocity field and the associated Stokes, Ekman and Rayleigh boundary layers on the plates are determined for the resonant and non-resonant cases. The ultimate steady state flows are examined for various cases. Rao et al., [1982] have made an initial value investigation of the combined free and forced convection effects in an unsteady hydromagnetic viscous, incompressible rotating fluid between two disks under a uniform transverse magnetic field. This analysis has been extended to porous boundaries by Sarojamma & Krishan [1981] and Sivaprasad [1985]. Mishra and Narayan [1986] have studied the unsteady free convective flow through a porous medium when the temperature of the plate is oscillating with time about a non-zero mean. Raptis [1986] has studied the unsteady MHD free convective flow of an electrically conducting fluid through a porous medium bounded by an infinite vertical porous plate. Sreeramachandra Murthy[1992] has investigated the MHD mixed convection flow of a viscous, electrically conducting fluid through a porous medium in a rotating parallel plate channel. The perturbations in the flow are created by a constant pressure gradient along the plates in addition to non-torsional oscillations of the lower plate. The exact solutions of the velocity and the temperature fields have been obtained by using the Laplace transform method.

Seth and Ghosh [1986] has investigated the unsteady hydromagnetic flow of a viscous, incompressible, electrically conducting fluid in rotating channel under the influence of periodic pressure gradient and of uniform magnetic field, which is inclined with the axes of rotation. The problem of steady laminar micro polar fluid flow through porous walls of different permeability had been discussed by Agarwal and Dhanpal [1987]. The steady and unsteady hydromagnetic flow of viscous incompressible, electrically conducting fluid under the influence of constant and periodic pressure gradient in the presence of magnetic field had been investigated by Ghosh [1991] to study the effect of slowly rotating systems with low frequency of oscillation when the conductivity of the fluid is low and the applied magnetic field is weak. El-mistikawy et al., [1990] have discussed the rotating disk flow in the presence of strong ; magnetic field and weak magnetic field. Later Hazem Ali Allia [1990] developed the MHD flow of in compressible ; viscous and electrically conducting fluid above an infinite rotating porous disk was extended to flow starting impulsively from rest. The fluid was subjected to an external uniform magnetic field perpendicular to the plane of the disk. The effects of uniform suction or injection through the disk on the unsteady MHD flow were also considered.

Recently Padmavati ea al [2008] et all have studied unsteady Hydromagnetic connected heat and mass transfer through a porous medium in a rotating channel. Circar and Mukherjee [2008] have analyzed the effect of mass transfer and rotation on a flow past a porous plate in a porous medium with variable suction in a slip flow regime.

Many processes in engineering areas occur at high temperatures and consequently the radiation plays a significant role. Chandrasekhara and Nagaru[1998] examined the composite heat transfer in a variable porosity medium bounded by an infinite vertical flat plate in the presence of radiation. Yih [1999] studied the radiation effects on natural convection over a cylinder embedded in porous media. Mohammadien and El-Amin [2000] considered the thermal radiation effects on power law fluids over a horizontal plate embedded in a porous medium. Raptis [2000] studied the steady flow and heat transfer in a porous medium with high porosity in the presence of radiation.

II. FORMULATION OF THE PROBLEM

We consider the steady flow of an incompressible, viscous fluid through a porous medium bounded by two parallel plates. In this undisturbed state both the plates and the fluid rotate with the same angular velocity Ω and are maintained at constant temperature and concentration. Further the plates are cooled or heated by constant temperature gradient in some direction parallel to the plane of the plates. We chose a Cartesian coordinate system O(x,y,z) such that the plates are at z=0 and z=L and the z-axis coinciding with the axis of rotation of the plates. We consider the Soret effect into account in the diffusion equation. The steady hydrodynamic boundary layer equations of motion including soret effect with respect to a rotating frame moving with angular velocity Ω under Boussinesq approximation are

$$-2\Omega v = -\frac{1}{\rho}\left(\frac{\partial p}{\partial x}\right) + \nu\left(\frac{\partial^2 u}{\partial z^2}\right) - \left(\frac{\nu}{k}\right)u - \left(\frac{\sigma\mu_e^2 H_o^2}{\rho}\right)u \qquad (2.1)$$

$$2\Omega u = -\frac{1}{\rho}(\frac{\partial p}{\partial y}) + \nu(\frac{\partial^2 v}{\partial z^2}) - (\frac{\nu}{k})v - (\frac{\sigma\mu_e^2 H_o^2}{\rho})v \qquad (2.2)$$

$$0 = --\frac{1}{\rho}(\frac{\partial p}{\partial z}) - g(1-\beta(T-T_0) - \beta^{\bullet}(C-C_0)) \qquad (2.3)$$

the energy equation is

$$(\frac{\partial}{\partial t} + u\frac{\partial}{\partial x} + v\frac{\partial}{\partial y})(T-T_0) = k_1\frac{\partial^2}{\partial z^2}(T-T_0) + (\frac{Q}{\rho_o C_p}) - \frac{\partial(q_r)}{\partial y} \qquad (2.4)$$

the diffusion equation is

$$(\frac{\partial}{\partial t} + u\frac{\partial}{\partial x} + v\frac{\partial}{\partial y})(C-C_o) = D_1\frac{\partial^2}{\partial z^2}(C-C_o) \qquad (2.5)$$

where u,v are the velocity components along x and y directions respectively, p is the pressure including the centrifugal force,ρ is the density, k is the permeability constant,μ is the coefficient of viscosity,k1 is the thermal diffusivity,D_1 is the chemical molecular diffusivity,β is the coefficient of thermal expansion ,β^* is the volumetric coefficient of expansion with mass fraction ,Q is the strength of the constant heat source,σ is the electrical conductivity and μe is the magnetic permeability of the medium. .

Invoking Rosseland approximation for radiative heat flux we get

$$q_r = -\frac{4\sigma^{\bullet}}{\beta_R}\frac{\partial(T'^4)}{\partial y}$$

and expanding T'^4 about Te by using Taylors expansion and neglecting higher order terms we get

$$T'^4 \cong 4T_e^3 T - 3T_e^4$$

Combining the equations(2.1) and (2.2) we obtain

$$-2i\Omega q = -\frac{1}{\rho}\ (\frac{\partial p}{\partial x} + i\frac{\partial p}{\partial y}) + \nu\ \frac{\partial^2 q}{\partial z^2} - (\frac{\nu}{k})q - (\frac{\sigma\mu_e^2 H_o^2}{\rho})q \qquad (2.6)$$

where

q = u+iv

Integrating equation (2.3) we obtain

$$\frac{p}{\rho} = -gz + \beta g\int(T-T_o)dz + \beta^{\bullet} g\int(C-C_o)dz + \phi(\xi,\bar{\xi}) \qquad (2.7)$$

where

$\xi = x - iy$, $\bar{\xi} = x + iy$

Using (2.7),equation(2.6) can be written as

$$-2i\Omega q - \nu\ \frac{\partial^2 q}{\partial z^2} + (\frac{\nu}{k})q + (\frac{\sigma\mu_e^2 H_o^2}{\rho})q = -2\beta g\frac{\partial}{\partial\xi}(T-T_o) - 2\beta^{\bullet} g\frac{\partial}{\partial\xi}(C-C_o) \qquad (2.8)$$

Since q = q(z, t) , equation (2.8) is valid if the temperature and concentration distributions are of the form

$T - T_0 = \alpha_1 x + \beta_1 y + \theta_1(z,t)$ (2.9a)

$C - C_0 = \alpha_2 x + \beta_2 y + \theta_2(z,t)$ (2.9b)

Where α_1 , β_1 ; α_2 , β_2 are the gradients of the temperature and concentration along 0(x, y) directions respectively , $\theta_1(z,t)$, $C_1(z,t)$ are the arbitrary functions of z and t. We taken $T_0 + \alpha_1 x + \beta_1 y + \theta_1 w_1$ and $T_0 + \alpha_1 x + \beta_1 y + \theta_1 w_2$, $C_0 + \alpha_2 x + \beta_2 y + C_1 w_1$ and $C_0 + \alpha_2 x + \beta_2 y + C_1 w_2$ to be temperature and concentration of the lower and upper plates respectively , for t > 0.

Substituting (2.7) in (2.6) and using (2.8) we get

$$2i\Omega q + (\frac{\nu}{k} + \frac{\sigma\mu_e^2 H_o^2}{\rho})q - \mu\frac{\partial^2 q}{\partial z^2} + \beta g\bar{A}z + \beta g\bar{B}z = D_2 \qquad (2.10)$$

Where $D_2 = \frac{\partial}{\partial \xi}[\phi(\xi', \bar{\xi}')]$, A= $\alpha_1 + i\,\beta_1$ and B = $\alpha_2 + i\,\beta_2$

Introducing non – dimensional variables (z , t , q , θ , c)

$$z' = \frac{z}{L}, \quad t' = \frac{t\nu}{L^2} \quad , \quad q' = \frac{t\nu}{L} \quad , \quad w' = \frac{wL^2}{\nu^2}$$

$$\theta' = \beta g L^3(\theta_1' - \theta_{1w_1}')/\nu^2, C' = \beta^{\bullet} g L^3(C_1' - C_{1w_1}')/\nu^2 \qquad (2.11)$$

the governing equations in the non – dimensional form (dropping the suffixes) are.

$$q_{zz} - (D^{-1} + 2iE^{-1} + M^2)q - q_t = G(1+N)z - R \qquad (2.12)$$

$$P(G_1 u + G_2 \upsilon) = \theta_{zz} + \alpha \qquad (2.13)$$

$$S_c(G_{1_c} u + G_{2_c} \mu) = C_{zz} \qquad (2.14)$$

where

$E = \frac{\nu}{L^2\Omega}$ (Ekmann number)

$M^2 = \frac{\sigma \mu_e^2 H_o^2 L^2}{\nu}$ (Hartman Number)

$D^{-1} = \frac{L^2}{k}$ (Darcy parameter)

$(G_1, G_2) = \frac{\beta G L^4}{\gamma^2}(\alpha_1, \beta_1)$ (Grashof numbers)

$(G_{1c}, G_{2c}) = \frac{\beta^* G L^4}{\gamma^2}(\alpha_2, \beta_2)$ (modified Grashof numbers)

$G = G_1 + G_2$

. $Gc = G_{1c} + G_{2c}$

$R = \frac{L^3 D}{\upsilon^2}$ (Reynolds number)

$N = \frac{\beta^* \Delta C}{\beta \Delta T}$ (Buoyancy ratio)

$P = \frac{\nu}{k_1}$ (Prandtl number)

$\alpha = \frac{QL^2}{k_1}$ (Heat Source parameter)

$Sc = \frac{\nu}{D}$ (Schmidt parameter)

III. SOLUTION OF THE PROBLEM

The governing equations (2.12)-(2.14) reduce to

$$\frac{d^2 q}{dz^2} - \lambda^2 q = (Gz - R) \qquad (2.15)$$

$$\frac{d^2\theta}{dz^2} + \alpha = P(G_1 u + G_2 v) \tag{2.16}$$

$$\frac{d^2C}{dz^2} - Sc(G_{1_c} u + G_{2_C} v) = 0 \tag{2.17}$$

$$\lambda^2 = D^{-1} + 2iE^{-1}, G1 = G(1+N)$$

The boundary conditions in the non-dimensional form are

$$\begin{aligned} q &= 0 \quad on \quad z = -1 \\ q &= 0 \quad on \quad z = -1 \\ \theta &= 0 \ , C = 0 \quad on \quad z = -1 \\ \theta &= \beta g L^3 (\theta_{1_{w_2}} - \theta_{1_{w_1}}) / \nu^2 = \theta_0 (say) \ \ on \ \ z = 1 \\ C &= \beta^* g L^3 (C_{1_{w_2}} - C_{1_{w_1}}) / \nu^2 = C_0 (say) \ \ on \ \ z = 1 \end{aligned} \tag{2.18}$$

Solving the equations (2.15)-(2.17) subject to the boundary conditions (2.18) we obtain

$$q = \frac{R}{\lambda^2}\left(\frac{Cosh(\lambda z)}{Cosh(\lambda)} - 1\right) + \frac{G}{\lambda^2}\left(\frac{Sinh(\lambda z)}{Sinh(\lambda)} - z\right)$$

$$\theta = GP\,\mathrm{Re}\,al\left(\frac{A_1}{\lambda^2}(Cosh(\lambda z) - Cosh(\lambda)) + \frac{A_2}{\lambda^2}(Sinh(\lambda z) - zSinh(\lambda)) - \right.$$

$$\left. - \frac{G}{6\lambda^2}(z^3 - z) - \frac{R}{2\lambda^2}((z^2 - 1)) + \alpha_1(z^2 - 1) + \frac{\theta_0}{2}(1 - z)\right)$$

$$C = A_5\,\mathrm{Re}\,al\left(\frac{A_1}{\lambda^2}(Cosh(\lambda z) - Cosh(\lambda)) + \frac{A_2}{\lambda^2}(Sinh(\lambda z) - zSinh(\lambda)) - \right.$$

$$\left. - \frac{G}{6\lambda^2}(z^3 - z) - \frac{R}{2\lambda^2}((z^2 - 1)) - A_6(z^2 - 1)/2\right)$$

IV. FLOW RATE, SHEAR STRESS, NUSSELT NUMBER AND SHERWOODNUMBER:

The non-dimensional flow rate is given by

$$Q = Q_x + iQ_y = \int_{-1}^{1} q\,dz$$

$$= \frac{2}{\lambda^2}(A_1 Sinh(\lambda) + R)$$

The Shear stress on the walls z = ±1 are given by

$$\tau = (\tau_x + \tau_y)_{\pm 1} = \left(\frac{dq}{dz}\right)_{\pm 1} = \lambda(\pm A_1 Sinh(\lambda) + A_2 Cosh(\lambda) - \frac{G}{\lambda^2}$$

The local rate of heat transfer across the walls (Nusselt Number) is given by

$$Nu = \left(\frac{d\theta}{dz}\right)_{z=\pm 1}$$

$$= GP\,\mathrm{Re}\,al\left((\pm A_1 Sinh(\lambda) + A_2 Cosh(\lambda))/\lambda \right.$$

$$\left. - \frac{G}{\lambda^2} \mp \frac{R}{\lambda^2}\right) \pm \alpha + A_3$$

The rate of mass transfer(Sherwood Number)is given by

$$Sh = (\frac{dC}{dz})_{z=\pm 1}$$
$$= A_5 \operatorname{Re} al((\pm A_1 Sinh(\lambda) + A_2 Cosh(\lambda))/\lambda - \frac{G}{\lambda^2} \mp \frac{R}{\lambda^2}) \mp A_6 + A_7$$

where

$$G_1 = G(1+N), A_1 = \frac{R}{\lambda^2 Cosh(\lambda)}, A_2 = \frac{G}{\lambda^2 Sinh(\lambda)}$$

$$A_3 = GPRl(\frac{G}{6\lambda^2} - \frac{A_2}{\lambda^2} Sinh(\lambda) - \frac{R}{2\lambda^2})$$

$$A_4 = -0.5\alpha + 0.5\theta - GPRl(\frac{A_1 Cosh(\lambda)}{\lambda^2} - \frac{R}{2\lambda^2})$$

$$A_5 = GNSc - \frac{ScSoGP}{N}, A_6 = \frac{ScSo\alpha}{N},$$

$$A_7 = A_5 Rl(\frac{G}{6\lambda^2} - \frac{A_2 Sinh(\lambda)}{\lambda^2}) + \frac{C_0}{2},$$

$$A_8 = A_5 Rl(-\frac{R}{\lambda^2} + \frac{A_1 Cosh(\lambda)}{\lambda^2}) + \frac{C_0}{2} + \frac{A_6}{2}$$

V. DISCUSSION OF THE NUMERICAL RESULTS

In this analysis we investigate the Soret and radiation effects on MHD connective heat and mass transfer of a viscous, electrically conducting fluid in a horizontal rotating channel.

The velocity, temperature and concentration profiles are drawn for different positive and negative G. It is to be noted that in all the profiles drawn we have taken G be real so that the applied pressure gradient in the oy-direction is zero and the applied pressure gradient in the ox-direction is positive or negative according as the walls are heated or cooled in the axial direction (i.e., G>0 or G<0). It is found from fig. 1 that in the heating of the channel walls the fluid changes its direction from positive to negative as we move from the lower half to the upper half there by indicating the reversal flow in the upper half of the channel. In the case of cooling (G<0) the reversal flow appears in the lower half. The region of reversal flow enlarges with increase in $|G|$ (<0>). Fig. 2 indicates the variation of u with D^{-1}, it follows that lesser the permeability of the porous medium. The variation of u with M shows that u exhibits a higher M (fig. 3) smaller the magnitude of u with M. Also an increase in the rotation parameter K reduces the magnitude of u (fig. 4). When the molecular buoyancy force dominates over the thermal buoyancy force $|u|$ enhancers in the entire fluid region when the forces act in the same direction and for the forces acting in opposite directions we find a reduction in $|u|$ in the flow region. (fig. 5). We find that for N>0 the region of reversal flow appears in the upper half region and for N<0 the flow continues to be negative except in the vicinity of the lower flow and this region of reversal flow extends towards the lower wall as $|N|$ increases (fig. 5). It is found that the velocity v exhibits a back flow and is directed towards the opposing the oy-direction near the lower wall for any value of G. For $|G|$ (<0) the velocity v experiences a back flow opposing oy-direction in the upper region. Also $|v|$ enhances with increase in $|G|$ (<0>) with a maximum at z = 0.6. The maximum v drifts towards the upper half for G>0 and for G<0 the point of maximum occurs at z = -06 and the maximum v enhances with G (fig. 6). Fig. 7 indicates that lesser the permeability of the porous medium smaller the magnitude of v. the behaviour of v with Hartmann number M exhibits a decreasing tendency in the entire flow region (fig. 8).

The variation of v with rotation parameter K exhibits that the fluid in the lower half is directed towards the mid region while it moves towards the upper wall (fig. 9). The variation of v with the buoyancy ratio N is shown in fig. 8. It is observed with $|V|$ enhances with N(>0) when the forces act in the same direction and depreciates with $|M|$ when the buoyancy forces act in opposite directions.

The temperature distribution (θ) is exhibited in figs. 10-13for different variations of the governing parameters. θ is positive or negative according as the actual temperature is greater or smaller than the equilibrium temperature. It is found that for G>0. θ is positive in the in the entire fluid region and for higher $|G|$ negative in the upper of and positive in lower half. But for higher $|G|$ it continues to be negative except in a narrow region adjacent to the lower wall (fig. 10). From fig 11 we find that lesser the permeability of the porous medium smaller the magnitude of the temperature for any G. The variation of θ with M shows that the temperature experiences a depreciation with increase in M (fig. 12). Also the effect of the radiation parameter N_1 is to enhance the temperature in the entire flow region (fig. 13). The variation of θ with rotation parameter k exhibits that the temperature continues to be positive for all values of k. The temperature experiences a marginal depreciation with increase in k (fig. 14). When the molecular buoyancy force dominates over the thermal buoyancy force the temperature enhances when the buoyancy forces act in the same direction and for different directions of the buoyancy forces θ decreases in the lower half and enhances in the upper half of the channel (fig. 15).

The concentration distribution (C) is positive for G>0 and negative for G<0. It is noticed that the concentration enhances with increase in G. Also for G<0 the concentration for $|G| \leq 2x10^3$ is negative in the entire fluid region and for higher $|G| \geq 3x10^3$. C is negative except in a narrow region abutting the lower wall $|C|$ enhances with $|G|$ (fig. 16). From fig. 17 we find that lesser the permeability of the porous medium smaller the concentration in the lower half and greater C in the right half. From fig. 14a shows that the concentration experiences a depreciation with increase in M (fig. 18). The variation of C with rotation parameter k indicates that for $k \leq 1$ it is totally positive and for higher $k \geq 1.5$, it is positive except in the vicinity of the lower wall and for further increase in k the transition from positive to negative extends towards the midregion). The variation of C with the buoyancy ratio N shows that C is positive for N = 1 and for higher values of N it is positive except in the region $0.6 \leq z \leq 0.8$, near the upper wall. For the buoyancy forces acting in opposite directions we find that the actual concentration is greater than the equilibrium concentration in the lower half and a reversed effect is observed in the upper half. Also $|C|$ enhances with increase in $|N|$(<0>)). The variation of C with S_c indicates that lesser the molecular diffusivity higher the concentration in the entire fluid region

The Shear stress (τ) at the walls $z = \pm 1$ has been evaluated for different governing parameters $G, D^{-1}, S_c, S_0, k, N, M$ and α are presented in tables. 1-8. The component of stress in the x-direction (τ_x) is positive in the heating case, and negative in the cooling case while τ_y is negative for G>0 and positive G<0. An increase in G enhances τ_x at both the walls. The variation of τ_x with D^{-1} shows that lesser. Permeability of the porous medium larger τ_x at z = -1 and smaller $|\tau_x|$ at z = 1. An enhancement in K depreicates τ_x at $z = \pm 1$. The variation of τ_y shows that enhances $|G|, D^{-1}$ and depreciates with M. An increase in $k \leq 1.5$ reduces $|\tau_y|$ and for further increase in $K \geq 2.5$, $|\tau_y|$ experiences an enhancement. When the molecular buoyancy force dominates over the thermal buoyancy force $|\tau_x|$ experiences an enhancement at walls when they act in the same direction and depreciates at z = 1 and enhances at z=-1 if they act in opposite directions. Also $|\tau_y|$ enhancement at $z = \pm 1$ with increase in $N_1>0$ while an increase in $N_1<0$, enhances $|\tau_y|$ at $z = \pm 1$ (tables – 8).

The Nusselt Number (N_u) which measures the rate of heat transfer across the walls $z = \pm 1$ has been exhibited in tables 9-12 for different variations of $N_1, G, D^{-1} M, k, N$ and α. It is found that the Nusselt Number (N_u) at $z = \pm 1$ is negative in both heating and cooling of the walls. The rate of heat transfer at both the walls enhances with G and depreciates with D^{-1}, M and k. An increase in the strength of the heat source is associated with an increase in N_u and an increase in $\alpha<0$ depreciates
$|N_u|$ at both the walls. When the molecular buoyancy force dominates over the thermal buoyancy force the magnitude of Nu at z = 1 depreciates when the buoyancy forces act in the same direction and enhances when they act in opposite directions.

The Sherwood Number (Sh) which measures the rate of mass transfer across the boundaries is depicted in tables 13-14 for different G.D.Sc.N and k. It is noticed that the Sherwood number (Sh) at the upper wall is negative and is positive at the lower wall for all variations. We find that an increase in G results in an enhancement at both the walls. The variation of Sh with D^{-1} and M shows that lesser thpermeability of the porous medium or higher the Lorentz force smaller $|Sh|$ at $z = \pm 1$. Alsosmaller the molecular diffusivity larger the magnitude of S_h at both the walls. Also an increase in the rotation parameter k

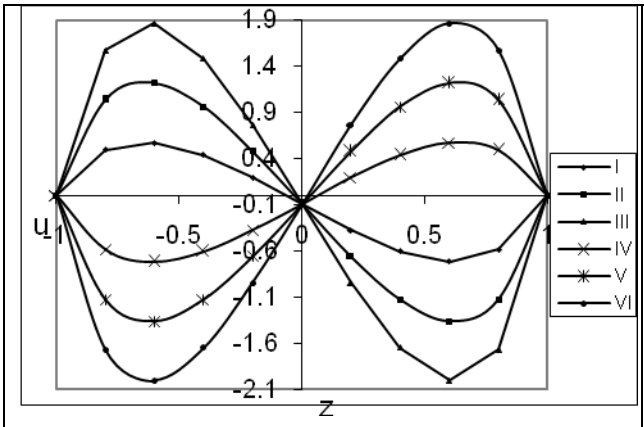

Fig.1 Variation of axial velocity u with G
$D^{-1}=10^3$, k= 50, N=1,Sc=1.30,S_0=0.50,α=2

	I	II	III	IV	V	VI
G	10^3	$2x10^3$	$3x10^3$	-10^3	$-3x10^3$	$-5x10^3$

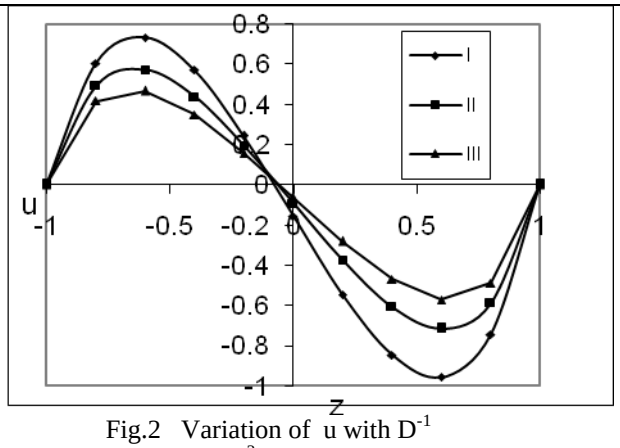

Fig.2 Variation of u with D^{-1}
$G=10^3$,k=50,N=1

	I	II	III
D^{-1}	$5x10^2$	10^3	$2x10^3$

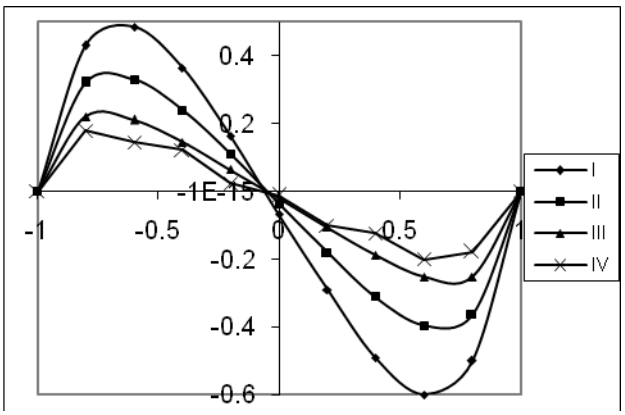

Fig.3 Variation of axial velocity(u) with M
$G=10^3$,$D^{-1}=10^2$

	I	II	III	IV
M	2	4	6	10

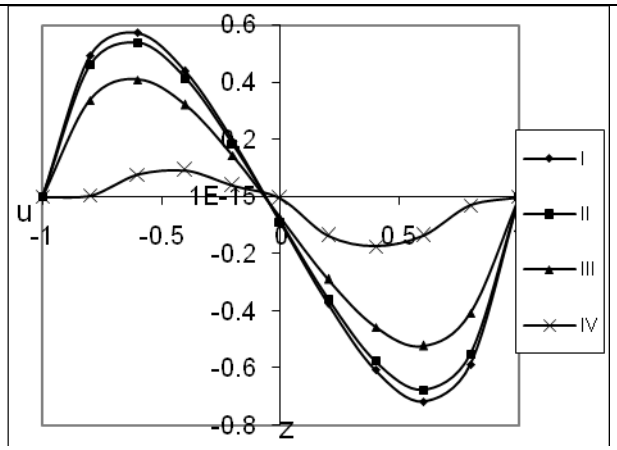

Fig.4 Variation of u with k
$G=10^3$,$D^{-1}=10^3$,N=1

	I	II	III	IV
k	0.5	1	1.50	2

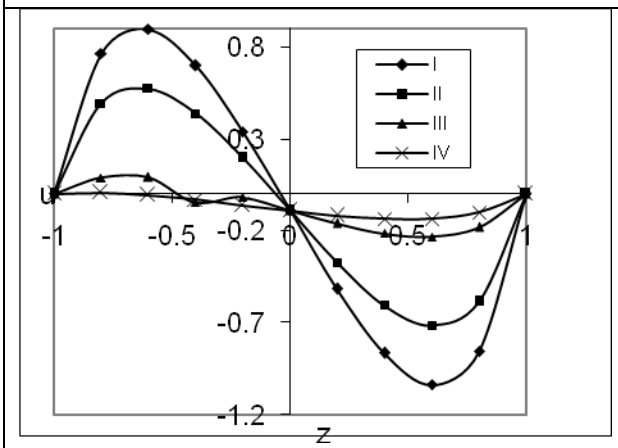

Fig.5 Variation of u with N
$G=10^3$, $D^{-1}=10^3$,k=.50

	I	II	III	IV
N	2	1	-0.5	-0.8

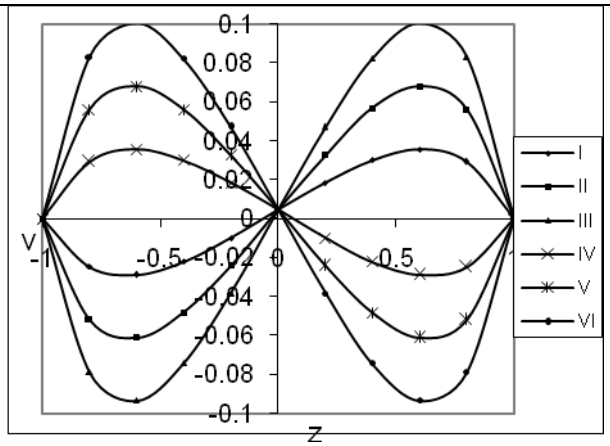

Fig.6 Variation of secondary velocity(v) with G
$D^{-1}=10^3$,k=0.5,N=1

	I	II	III	IV	V	VI
G	10^3	$2x10^3$	$3x10^3$	-10^3	$-2x10^3$	$-3x10^3$

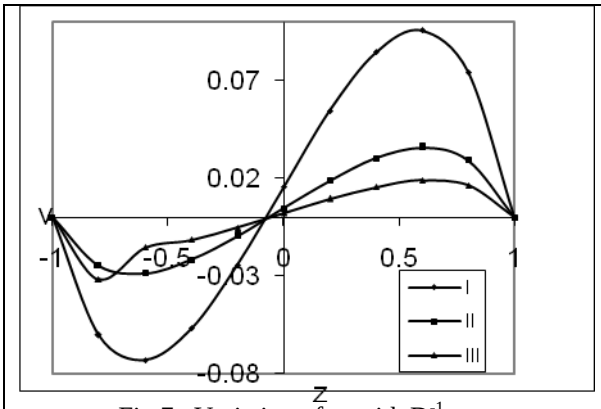

Fig.7 Variation of v with D^{-1}
$G = 10^3$, k=.50, N=1

	I	II	III
D^{-1}	$5x10^2$	10^3	$2x10^3$

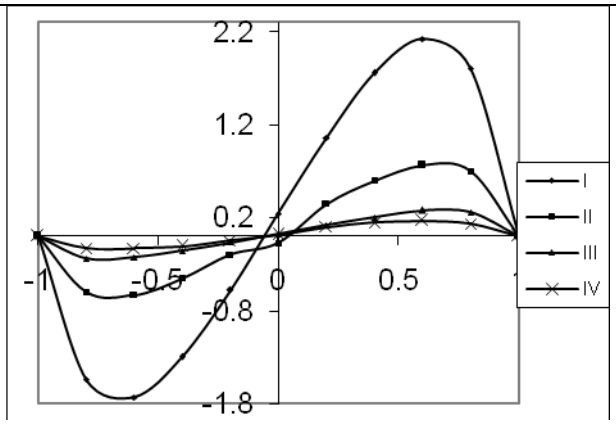

Fig.8 Variation of v with M
$G=10^3$, N=1, Sc=1.3

	I	II	III	IV
M	2	4	6	10

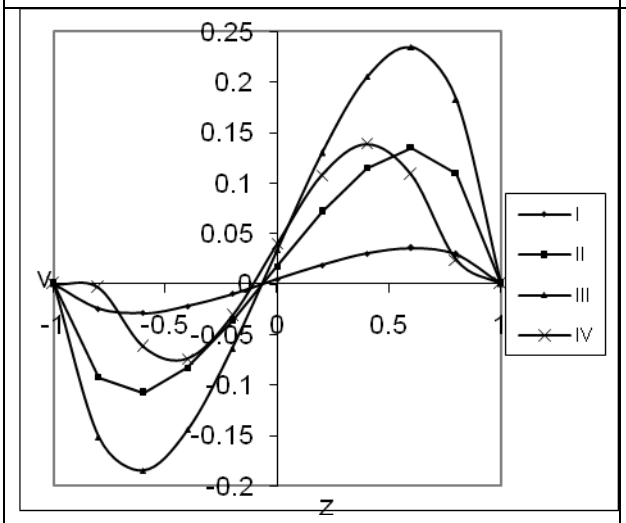

Fig.9 Velocity v with k
$G=10^3$, $D^{-1}=10^3$, N=1

	I	II	III	IV
k	0.5	1	1.50	2

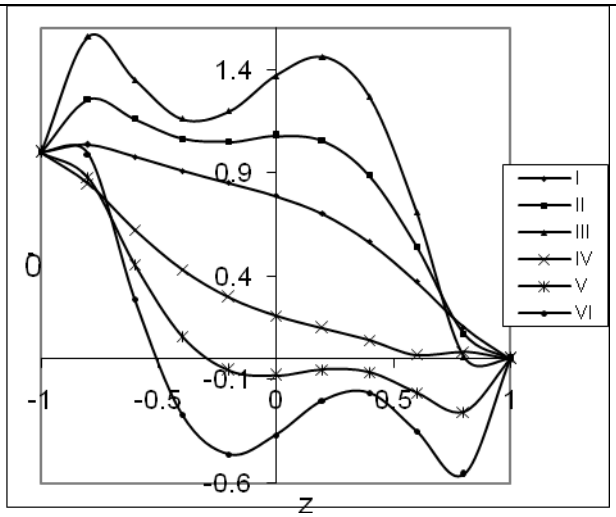

Fig.10 Variation of temperature(θ)with G
$G=10^3$, $D^{-1}=10^3$, k=.5, N=1

	I	II	III	IV	V	VI
G	10^3	$2x10^3$	$3x10^3$	-10^3	$-2x10^3$	$-3x10^3$

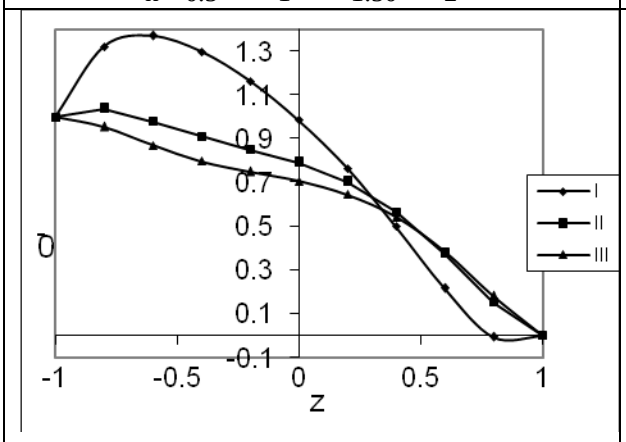

Fig.11 Variation of temperature(θ)with D^{-1}
$G=10^3$, $D^{-1}=10^3$, k=.5, N=1

	I	II	III	IV	V	VI
G	10^3	$2x10^3$	$3x10^3$	-10^3	$-2x10^3$	$-3x10^3$

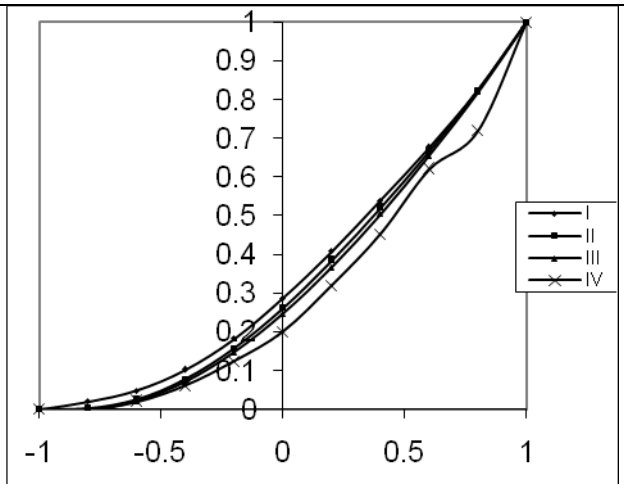

Fig.12Variation of temperature (θ) with M

	I	II	III	IV
M	2	4	6	10

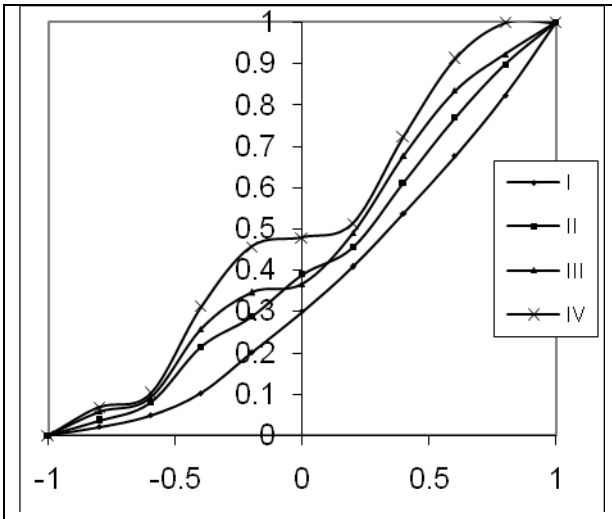

Fig.13 Variation of θ with N1

	I	II	III	IV
N1	0.5	1.5	5	10

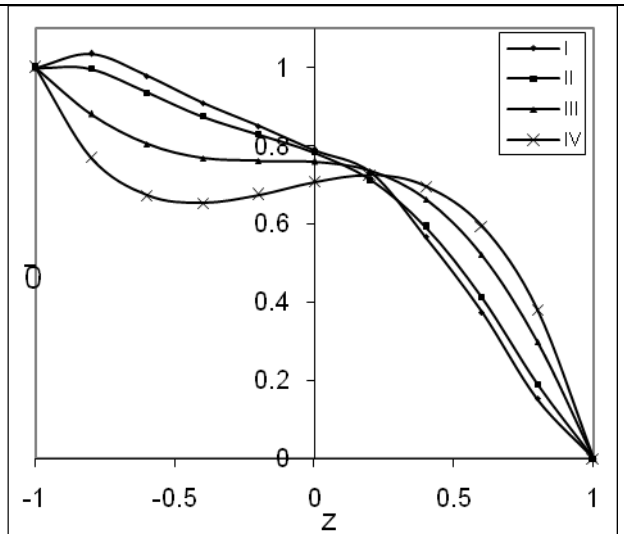

Fig.14 Temperature θ with k
$G=10^3, D^{-1}=10^3, N=1, M=2$

	I	II	III	IV
k	0.5	1	1.5	2

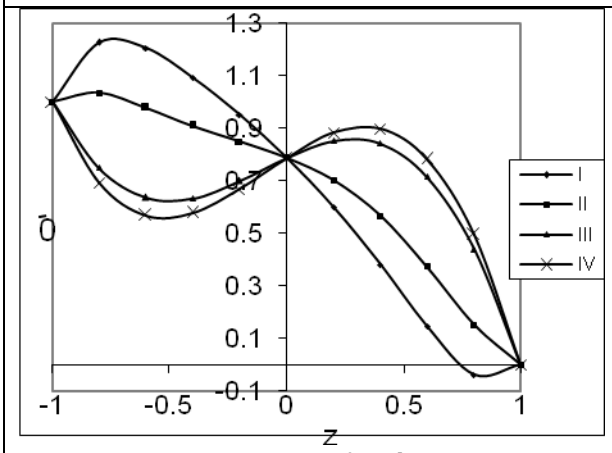

Fig.15 Temperature θ with N
$G=10^3, D^{-1}=10^3, k=0.50$

	I	II	III	IV
N	2	1	-0.5	-0.8

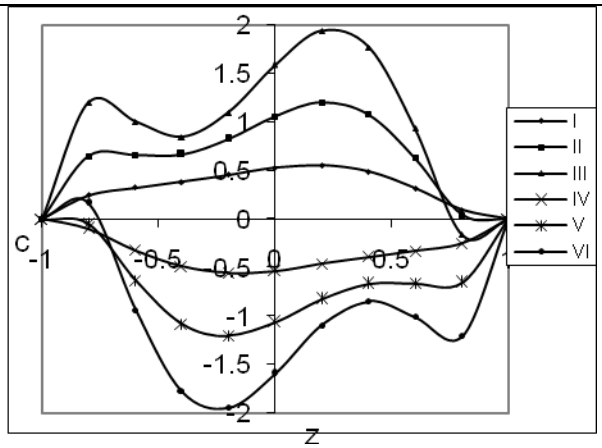

Fig.16 Variation of Concentration(C) with G
$D^{-1}=10^3, k=0.5, N=1, M=2$

	I	II	III	IV	V	VI
G	10^3	$2x10^3$	$3x10^3$	-10^3	$-2x10^3$	$-3x10^3$

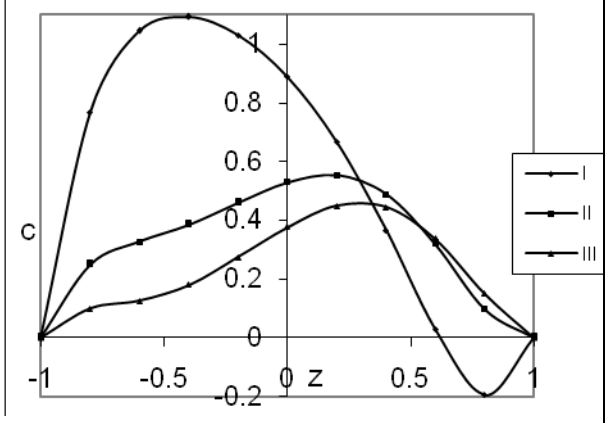

Fig.17Variation of C with D^{-1}
$G=10^3, k=0.5, N=1$

	I	II	III
D^{-1}	$5x10^2$	10^3	$2x10^3$

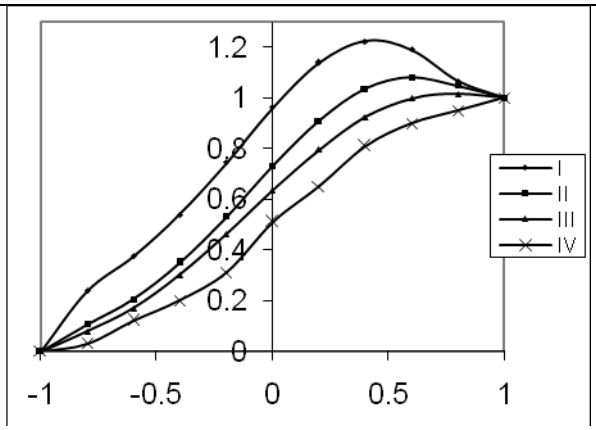

Fig.18 Variation of C with M
$G=10^3, N=1, Sc=1.3$

	I	II	III	IV
M	2	4	6	10

Table.1
Shear Stress (τ) at z = 1
P=0.71,N=1,α=2

G/ τ	I	II	III	IV	V	VI	VII
10^3	4.76054	3.44816	2.84281	4.36155	3.48124	4.75752	4.73719
$3x10^3$	9.42302	6.82630	5.62827	8.63367	6.89176	9.41705	9.37685
-10^3	-4.56442	-3.30813	-2.72810	-4.18267	-3.33982	-4.56154	-4.54213
$-3x10^3$	-9.22691	-6.68627	-5.51356	-8.45478	-6.75034	-9.18178	-9.18178

Table.2
Shear Stress (τ) at z = -1

G/ τ	I	II	III	IV	V	VI	VII
10^3	4.56442	3.30813	2.72810	4.18267	3.33982	4.54154	4.54213
$3x10^3$	9.22691	6.68627	5.51356	8.45478	6.75034	9.22107	9.18178
-10^3	-4.76054	-3.44816	-2.84281	-4.36155	-3.48124	-4.75752	-4.73719
$-3x10^3$	-9.42302	-6.62630	-5.62827	-8.63367	-6.89176	-9.41705	-9.37685

Table.3
Shear Stress ($\tau_y x10$) at z = 1

G/ τ	I	II	III	IV	V	VI	VII
10^3	-0.1087	-0.04082	-0.0227	-0.0832	-0.0420	-0.9769	-2.6937
$3x10^3$	-0.21502	-0.08072	-0.0449	-0.1647	-0.0830	-1.9325	-5.3291
-10^3	0.1039	0.0390	0.0218	0.0797	0.0402	0.9345	2.5769
$-3x10^3$	0.2121	0.0789	0.0440	0.1611	0.0813	1.8901	5.2123

Table.4
Shear Stress (τ_y x10) at z = -1

G/ τ	I	II	III	IV	V	VI	VII
10^3	-0.1039	-0.3900	-0.0218	-0.0797	-0.0402	-0.9345	-2.5769
$3x10^3$	-0.2102	-0.0789	-0.0440	-0.1611	-0.0813	-1.8900	-5.2123
-10^3	0.1087	0.0408	0.0227	0.0832	0.0420	0.9769	2.69937
$-3x10^3$	0.2150	0.0807	0.0449	0.1647	0.0830	1.9325	5.32913

D^{-1}	10^3	$3x10^3$	$5x10^3$	10^3	10^3	10^3	10^3
M	2	2	2	5	10	2	2
K	0.5	0.5	0.5	0.5	0.5	1.5	2.5

Table.5
Shear Stress (τ_x) at z = 1
P=0.71,$D^{-1}=10^3$,M=2,α=2

G/ τ	I	II	III	IV
10^3	4.76054	7.21197	1.08339	0.88657
$3x10^3$	9.42302	14.3258	2.06873	1.87660
-10^3	-4.56442	-7.0158	-0.88728	-0.76549
$-3x10^3$	-9.22691	-14.1297	-1.87262	-1.65784

Table.6
Shear Stress (τ_x) at z = -1

G/ τ	I	II	III	IV
10^3	4.56442	7.01585	0.88728	1.02346
$3x10^3$	9.22691	14.12977	1.87262	2.06548
-10^3	-4.76054	-7.21197	-1.08339	-1.13478
$-3x10^3$	-9.42302	-14.3258	-2.06873	-2.35456

Table.7
Shear Stress (τ_y x10) at z = 1

G/ τ	I	II	III	IV
10^3	-0.1087	-0.1676	-0.0203	-0.02456
$3x10^3$	-0.21502	-0.3328	-0.0382	-0.36785
-10^3	0.1039	0.16293	0.0156	0.02341
$-3x10^3$	0.2121	0.32812	0.0335	0.03678

Table.8
Shear Stress (τ_y x10) at z = -1

G/ τ	I	II	III	IV
10^3	-0.1039	-0.1629	-0.01563	-0.01254
$3x10^3$	-0.2102	-0.3281	-0.03352	-0.03045
-10^3	0.1087	0.1676	0.02033	0.018765
$-3x10^3$	0.2150	0.3328	0.03822	0.032679

	I	II	III	IV
N	1	2	-0.5	-0.8

Table.9
Nusselt Number(Nu) at z = 1
P=0.71,N=1,α=2

G/ τ	I	II	III	IV	V	VI	VII
10^3	-0.43197	-0.01321	0.17801	-0.28479	0.00343	-0.43055	-0.42095
$3x10^3$	-3.28032	-1.53938	-0.89431	-2.70498	-1.57767	-3.27472	-3.23726
-10^3	-0.34801	0.05735	-0.20803	-0.21426	0.04841	-0.34672	-0.33806
$-3x10^3$	-3.11237	-1.45111	-0.83426	-2.56393	-1.4877	-3.10707	-3.07150

Table.10
Nusselt Number(Nu) at z = - 1

G/ τ	I	II	III	IV	V	VI	VII
10^3	-5.27604	-3.78972	-3.23722	-4.78562	-3.82249	-5.27131	-4.53213
$3x10^3$	-15.4120	-9.32074	-7.05897	-13.4010	-9.45490	-15.3926	-15.2621
-10^3	-5.58391	-3.95156	-3.34730	-5.04422	-3.98744	-5.57867	-5.54347
$-3x10^3$	-16.0277	-9.82630	-7.27912	-13.9182	-9.78479	-16.0073	-15.8699

	I	II	III	IV	V	VI	VII
D^{-1}	10^3	$3x10^3$	$5x10^3$	10^3	10^3	10^3	10^3
M	2	2	2	5	10	2	2
K	0.5	0.5	0.5	0.5	0.5	1.5	2.5

Table.11
Nusselt Number(Nu) at z = 1
P=0.71,$D^{-1}=10^3$,M=2,α=2

G/ τ	I	II	III	IV	V	VI
10^3	-0.43197	-0.6789	-1.4567	0.45367	0.34675	0.30246
$3x10^3$	-3.28032	-3.98765	-4.35768	2.54688	2.12348	1.89765
-10^3	-0.34801	-0.37865	-0.45673	0.33245	0.30132	0.28976
$-3x10^3$	-3.11237	-3.23452	-3.65788	3.23489	2.98763	2.45638

Table.12
Nusselt Number(Nu) at z = -1

G/ τ	I	II	III	IV	V	VI
10^3	-5.27604	-5.78965	-6.12347	4.56785	4.12343	3.76552
$3x10^3$	-15.4120	-15.8775	-15.9998	13.2345	12.8976	11.8977
-10^3	-5.58391	-5.90876	-6.23414	5.12543	4.98765	4.45678
$-3x10^3$	-16.0277	-17.1234	-17.8976	14.6789	14.0123	12.7886

	I	II	III	IV	V	VI
α	2	4	6	-2	-4	-6

Table.12
Nusselt Number(Nu) at z = 1
P=0.71,$D^{-1}=10^3$,M=2,α=2

G/ τ	I	II	III	IV	V
10^3	-0.43197	-0.5678	-1.2365	-1.6785	-1.9876
$3x10^3$	-3.28032	-3.6785	-5.67854	-5.9876	-6.0123
-10^3	-0.34801	-0.39876	-0.6785	-0.7896	-0.9987
$-3x10^3$	-3.11237	-3.4567	-4.3568	-4.9876	-5.1232

Table.13
Nusselt Number(Nu) at z = -1

G/ τ	I	II	III	IV	V
10^3	-5.27604	-5.1234	-4.6785	-4.3456	-3.5674
$3x10^3$	-15.4120	-14.678	-13.8976	-13.0123	-12.786
-10^3	-5.58391	-5.7654	-5.4578	-4.9876	-4.2345
$-3x10^3$	-16.0277	-15.678	-15.4589	-14.5687	-13.345

	I	II	III	IV	V
N1	0.5	1.5	4	10	100

Table.15
Sherwood Number(Sh) at z = 1
P=0.71,N=1,α=2

G/ τ	I	II	III	IV	V	VI	VII
10^3	-5.41026	-2.94852	-2.03902	-4.59460	-3.00251	-5.40224	-5.34838
$3x10^3$	-21.0773	-11.4977	-7.95454	-17.9049	-11.7081	-21.0462	-20.8372
-10^3	-4.84655	-2.65220	-1.83747	-4.12111	-2.70049	-4.83959	-4.79194
$-3x10^3$	-19.9499	-10.9051	-7.55144	-16.9579	-11.1039	-19.9207	-19.7242

Table.16
Sherwood Number(Sh) at z = - 1

G/ τ	I	II	III	IV	V	VI	VII
10^3	0.02779	0.00806	0.00380	0.01992	0.00836	0.24975	0.68673
$3x10^3$	0.10860	0.03154	0.01488	0.07789	0.03273	0.97597	2.68370
-10^3	0.02523	0.00736	0.00348	0.01812	0.00764	0.22672	0.62435
$-3x10^3$	0.10348	0.03015	0.01424	0.07429	0.03128	0.92992	2.55724

	I	II	III	IV	V	VI	VII
D^{-1}	10^3	$3x10^3$	$5x10^3$	10^3	10^3	10^3	10^3
M	2	2	2	5	10	2	2
K	0.5	0.5	0.5	0.5	0.5	1.5	2.5

REFERENCES

[1] Agarwal R.S and Dhanapal. C(1987) : Numerical solution to the flow a micro- polar fluid flow through porous walls of different permeability, Int. J. Engg. Sci, V. 25, No. 30, pp 325-336

[2] Claire Jocobs – Q(1971), : Jour Maths. Appl. Maths, V. 24, p. 221

[3] Cirac and Mukherjee(2008) : Acta Ciencia Indica V. 24. M 202, No. 2, pp 737- 751

[4] Chandra Sekhara B.C and Nagaraju P(1998) : Composite heat transfer in the case of a steady laminar flow of a gray fluid with small optical density past a horizontal plate embedded in a porous medium, Warme stoffubentras, V 23 (6) pp. 243-352

[5] Debnath. L(1975) : ZAMM V. 55 p 431

[6] El. Mistikawy T.M.A Attia H.A (1990) The rotating disk flow in the presence of strong magnetic field, Proc 3rd Int. Congr of fluid mechanics, Cairo, Egypt,V. 3, 2 – 4, pp 1211-1222

[7] Ghouse S.K. (1991) : A note on steady and unsteady hydromagnetic flow in rotating channel in the presence of inclined magnetic field, Int. J. Engg. Sci, V. 29, No. 8 ; pp 1013-1016

[8] Hazem Ali Attia(1990) : Unsteady MHD flow near a rotating porous disk with uniform suction or injection. Fluid dynamics Research V. 23, pp 283-290

[9] J. Atmo's(1966): Sci. 23. p. 54

[10] Lugt H.J. and Schwidesk E.W (1965): Q. Appl. Maths. 23, p. 130

[11] Mohammeaden A.A. and El. Amin M.F(2000) : Thermal radiation effects on power – law fluids over a horizontal plate embedded in a porous medium, Int. com Heat Mass V. 127 (2), pp. 1025-1035
[12] Murthy K.N.V(1979) : Appl. Sci. Res, V. 35, p 111
[13] Prabhamani Patil and Vaidyanathan G(1984) : Prog. Sci, V. 21, No. 2, p. 123
[14] Cheng P(1978) : Heat Transfer in Geothermal Systems, Advances in Heat Transfer, V. 14, Academic Press. New York, pp 1-105 Padmavathi, A(2008) : Acta Ciencia Indica V. 34, No. 2, pp 871-888
[15] Raptis A.A(2000) : Radiation and flow through a porous medium, J. porous media. V. 4, pp 271-273
[16] Rao D.R.V.P. Krishna D.V and Debnath. L (1982) : Acta Mech, V. 143, p. 49
[17] Raptis A.A(1986) : Energy Res., V. 10, p. 97
[18] Sarojamma G. and Krishna D.V (1981): Acta Mech V. 39, p. 277
[19] Singh. P, Mishra J.K. and Narayana K.A(1986) : Int. J. Engg Sci., V. 24, No. 2, p. 277
[20] Siva Prasad R(1985) : Convection flow in magnetohydro dynamics, Ph.D thesis, p. 101 S.K. University Anantapur
[21] Sree Ramachandra Murthy, A(1992) : Bouyancy induced hydromagnetic flows through a porous medium Ph.D thesis, p. 125, S.K. University Anantapur, India
[22] Seth G.S. and S.K. Ghosh(1986) : Int. J. Engg. Sci. V. 24, Issue 7, pp. 1183-1193
[23] Yih., K.A(1999) : Radiation effects on natural convection over a vertical cylinder embedded in a porous media, Int. Com Heat Mass transfer, V. 26 (2), pp. 259-267